Molecular Cell, Volume *34*

Supplemental Data

High-Affinity Binding of Chp1 Chromodomain to K9 Methylated Histone H3 Is Required to Establish Centromeric Heterochromatin

Thomas Schalch, Godwin Job, Victoria J. Noffsinger, Sreenath Shanker, Canan Kuscu, Leemor Joshua-Tor, and Janet F. Partridge

Supplemental Experimental Procedures

Peptide binding assays

Fluorescence polarization binding assays.

Fluorescence polarization (FP) experiments were carried out using a Biotek Synergy 4 plate reader (Biotek) at 30°C following the procedure described previously (Jacobs et al. 2003). 10 nM of fluorescein labeled peptide (synthesized as Flu-ARTKQTARK^{meX}STGGKAY, Peptide Protein Research Ltd, UK) with varying methyl marks on K9 was incubated for 30 min at 30°C with varying amounts of chromodomain protein in binding buffer (50 mM KPO_4 pH 7.0, 25 mM NaCl, 1 mM DTT, 100 µg/ml BSA (NEB)). BSA was included to prevent aggregation of the peptide and was confirmed not to interfere with the binding measurements.

Concentration of proteins was measured by absorbance spectroscopy (Swi6: ε_{280} = 41,035 $M^{-1}cm^{-1}$, Chp1 CDs: ε_{280} = 29,450 $M^{-1}cm^{-1}$, Clr4 CD: ε_{280} = 20,970 $M^{-1}cm^{-1}$,). Peptide concentrations were determined using absorbance spectroscopy (extinction coefficient for tyrosine, ε_{280} = 1280 $M^{-1}cm^{-1}$; extinction coefficient for fluoresceinated peptides ε_{492} = 68,000 $M^{-1}cm^{-1}$). Binding curves were analyzed using the scipy module of the python programming language. Data was analyzed as described (Jacobs et al. 2003), except that a bimodal equation to account for non-specific binding at high protein concentrations was used when the data displayed clear bimodal behavior:

$$f(A) = A_0 + (A_s - A_0)\left[\frac{x}{K_{ds}x}\right] + (A_{ns} - A_s)\left[\frac{x}{K_{dns}x}\right]$$

With x being the protein concentration, A_0 the anisotropy of the free peptide, A_s the anisotropy of the specifically bound peptide and A_{ns} the anisotropy of the non-specifically bound peptide. K_{ds} represents the specific dissociation constant and K_{dns} the non-specific dissociation constant.

Isothermal Titration Calorimetry

Isothermal titration calorimetry was performed on a VP-ITC instrument (MicroCal). Chromodomain proteins and peptides (same sequence as for FP, but without label) were dialyzed overnight against 50 mM KPO_4 pH 7.0, 25 mM NaCl, 1 mM DTT. Exothermic heats of reaction (µcal/s) were measured for 30 injections of the H3 peptides (250 µM), each 10µl, spaced at 4 min intervals, into 1.41 ml of 25 µM chromodomain protein. Binding curves were analyzed by non-linear least squares fitting of the data using the Origin (MicroCal) software package.

Crystal structure determination

Data were collected under cryo conditions at the National Synchrotron Light Source (NSLS) beam line X29 using a wavelength of 1.0809 Å. Phases were obtained by molecular replacement using the HP1 chromodomain (Jacobs et al. 2002) excluding the peptide (chain A of PDB entry 1KNE) as a search model. The structure was built in coot (Emsley et al. 2004) and refined with phenix.refine (Adams et al. 2002). The final model shows Ramachandran statistics of 90.7% of all residues in most favored and 9.3% in additionally allowed regions as calculated by Procheck. Coordinates can be accessed under PDB code 3G7L.

We observed a crucial crystal contact mediated by zinc ions that are coordinated by a total of four aspartates; D48 and D51 from two separate molecules related by crystallographic symmetry. These residues were simultaneously mutated to serine to investigate a potential role for the zinc binding motif. The recombinant chromodomain for this mutant was completely insoluble, and therefore an affinity could not be determined for this mutant.

Strain construction.

Mutagenesis of the Chp1 chromodomain was performed by homologous recombination to replace the *ura4* marker in PY 282 (*CDΔ::ura4*$^+$*chp1-6xmyc* (Petrie et al. 2005)) with a chimeric PCR product consisting of the chromodomain point mutant of interest. Strains were selected on FOA medium, and PCR and DNA sequencing were used to confirm the generation of the mutant *chp1-6xmyc* strains after two outcrosses. Strains were outcrossed again to introduce the centromeric *ura4*$^+$ marker at *otr1R(Sph1)* and the *ura4* minigene (*ura4 DS/E*) at the endogenous *ura4* locus. The Chp1 chromodomain series was similarly generated in strains lacking the C terminal 6xmyc tag on Chp1. For these strains, *ura4* was used to replace the chromodomain of Chp1 in PY42 (generating PY

3054), and following generation of the Chp1 point mutants, strains were outcrossed twice with PY90 prior to outcrossing with PY189 and reverification of the mutation by sequencing.

To test whether Chp1 chromodomain mutations affect heterochromatin establishment, the *clr4* null allele (*clr4Δ::KanR*) was introduced by crossing into strains bearing *chp1* chromodomain mutant alleles lacking the 6xmyc tag. *clr4*$^+$ was then reintegrated into the *clr4Δ* genomic locus by transformation with a plasmid bearing a genomic clone of *clr4*$^+$ (JP1084, Partridge et al., 2007) which had been linearized by digestion with HpaI. Strains that were correctly targeted, with a single site of integration of *clr4*$^+$ at the *clr4Δ* genomic locus were identified by PCR and Southern analysis, and further characterization (serial dilution, RNA and ChIP analyses) was then performed on two independent *clr4*$^+$ reintegration strains for each *chp1* allele.

To test whether high copy *clr4*$^+$ could compensate for the establishment defect, strains lacking *clr4* and bearing the untagged *chp1* alleles were transformed with JP1078, a multicopy *his3*$^+$ vector carrying a genomic clone of *clr4*$^+$, or the empty *his3*$^+$ vector JP1049 (Partridge et al., 2007). Following transformation, the vector was maintained in cells by selection on media lacking histidine.

Supplementary References

Adams, P. D. et al. (2002). PHENIX: building new software for automated crystallographic structure determination. Acta Crystallogr. D Biol. Crystallogr. *58*, 1948-54.

Emsley, P., and Cowtan, K. (2004). Coot: model-building tools for molecular graphics. Acta Crystallogr. D Biol. Crystallogr. *60*, 2126-32.

Jacobs, S. A., Fischle, W., and Khorasanizadeh, S. (2003). Assays for the Determination of Structure and Dynamics of the Interaction of the Chromodomain with Histone Peptides. In Chromatin and Chromatin Remodeling Enzymes, Part B Methods in enzymology. (Academic Press), pp. 131-148.

Jacobs, S. A., and Khorasanizadeh, S. (2002). Structure of HP1 Chromodomain Bound to a Lysine 9-Methylated Histone H3 Tail. Science *295*, 2080-2083.

Partridge, J. F., DeBeauchamp, J. L., Kosinski, A. M., Ulrich, D. L., Hadler, M. J., and Noffsinger, V. J. (2007). Functional Separation of the Requirements for Establishment and Maintenance of Centromeric Heterochromatin. Mol. Cell *26*, 593-602.

Petrie, V. J., Wuitschick, J. D., Givens, C. D., Kosinski, A. M., and Partridge, J. F. (2005). RNA Interference (RNAi)-Dependent and RNAi-Independent Association of the Chp1 Chromodomain Protein with Distinct Heterochromatic Loci in Fission Yeast. Mol. Cell. Biol. *25*, 2331-2346.

Table S1. Summary of the ITC data

Protein	Peptide	T(C)	K_d (μM)	ΔH (kcal/mol)	N	ΔG (kcal/mol)	TΔS (kcal/mol)
Chp1 CD wt	H3K9me3	27	0.30	-28.70	0.90	-8.95	-19.75
Chp1 CD wt	H3K9me2	27	0.74	-29.10	0.94	-8.42	-20.68
Swi6	H3K9me3	27	1.69	-14.42	0.85	-7.91	-6.51
Swi6	H3K9me2	27	3.38	-14.40	0.93	-7.50	-6.90

Table S2. Binding constants (K_d) to S10 phosphorylated di- and trimethylated H3K9 peptides in μM for Chp1 CD and Swi6

	Chp1 CD WT*	**Swi6***
H3K9me2 S10P	278.76 ± 115.62	228.20
H3K9me3 S10P	105.93 ± 37.32	59.52

* Data for Chp1 represent mean of 2 experiments ± standard deviation, and a single experiment is shown for Swi6

Table S3. Chromosome missegregation frequency in Chp1 mutant strains

Background strain	No. anaphase cells screened	No. cells with lagging chromosomes (%)*	Strain no.
chp1Δ	103	24 (23.3)	PY90
chp1-6xmyc	101	1 (<1)	PY189
E23Vchp1-6xmyc	100	0 (<1)	PY760
V24Mchp1-6xmyc	101	1 (<1)	PY630
E23V,V24Mchp1-6xmyc	103	3 (2.9)	PY1681
N59Achp1-6xmyc	104	3 (2.8)	PY631
V21Achp1-6xmyc	103	3 (2.9)	PY3086
F61Achp1-6xmyc	100	0 (<1)	PY3141
D48S,D51Schp1-6xmyc	102	1 (<1)	PY3091
swi6CDchp1-6xmyc	101	1 (<1)	PY3393
V24Rchp1-6xmyc	107	25 (23.4)	PY3107

*****Frequency of lagging chromosomes on late-anaphase spindles (>5 μm) was determined by staining with anti–alpha tubulin antibodies; DNA was visualized by DAPI staining.

Table S4. Chromosome segregation analysis during establishment of heterochromatin

Background strain	No. anaphase cells screened	No. cells with lagging chromosomes (%)*	Strain no.
wild-type	101	1 (<1%)	PY2036
clr4Δ	209	39 (18.7)	PY1838
clr4Δ to clr4+	152	7 (4.6)	PY3417
E23Vchp1, clr4Δ to clr4^{+}	210	17 (8.1)	PY3409
V24Mchp1, clr4Δ to clr4^{+}	203	31 (15.3)	PY3413
N59Achp1, clr4Δ to clr4^{+}	109	12 (11)	PY3429
F61Achp1, clr4Δ to clr4^{+}	108	1 (<1)	PY3421
D48S, D51Schp1, clr4Δ to clr4^{+}	163	9 (5.5)	PY3401
swi6CDchp1, clr4Δ to clr4^{+}	145	6 (4.1)	PY3425

*****Frequency of lagging chromosomes on late-anaphase spindles (>5 μm) was determined by staining with anti–alpha tubulin antibodies; DNA was visualized by using DAPI.

Table S5. Genotypes of fission yeast strains used in this analysis

Fig 3A	Py 396	h+ otr1R (Sph1)::ura4 ura4DS/E chp1::chp1-6xmyc -LEU2 ade6-210 leu1-32
	Py 225	h90 otr1R (SphI)::ura4 ura4DS/E chp1::his3+ ade6-210 leu1-32 his3+
	Py 362	h+ otr1R (SphI)::ura4 ura4DS/E chp1::N59Achp1-6xmyc-LEU2 ade6DN/N or -210 leu1-32
	Py 357	h+ otr1R (Sph1)::ura4 ura4DS/E chp1::V24Mchp1-6xmyc-LEU2 ade6DN/N or -210 leu1-32
	Py 795	h+ otr1R (Sph1)::ura4 ura4DS/E chp1::E23Vchp1-6xmyc-LEU2+ ade6-210 leu1-32
	Py 905	h+ otr1R Sph1::ura4 ura4DS/E chp1::E23V,V24Mchp1-6xmyc-LEU2 ade6-210 leu1-32
	Py 3166	h- otr1R (Sph1)::ura4 ura4-DS/E chp1::V24Rchp1-6xmyc-LEU2 ade6-210 leu1-32
	Py 3129	h- otr1R (Sph1)::ura4 ura4-DS/E chp1::V21Achp1-6xmyc-LEU2 ade6-210 leu1-32
	Py 3188	h? otr1R (Sph1)::ura4 ura4-DS/E chp1::F61Achp1-6xmyc-LEU2 ade6-210 leu1-32
	Py 3132	h- otr1R (Sph1)::ura4 ura4-DS/E chp1::D48S,D51Schp1-6xmyc-LEU2 ade6-210 leu1-32
	Py 3462	h? otr1R (Sph1)::ura4 ura4DS/E chp1::chp1$_{aa1-8}$Swi6CD$_{aa68-132}$chp1$_{aa71-960}$-6xmyc-LEU2 ade6-210 leu1-32 arg3D? his3D?
Fig. 3B, 3C, 4A,4B,4C, S3,S4,S5,S6 ,S7	Py 42	h- ura4-D18 ade6-210 leu1-32 arg3D his3D
	Py 189	h- chp1::chp1-6xmyc-LEU2 ura4D18 ade6-210 leu1-32 arg3D his3D
	Py 1798	h- clr4Δ::KanR ura4D18 or DS/E ade6-210 leu1-32 arg3D his3D
	PY 90	h- chp1Δ::his3+ ura4DS/E ade6-210 leu1-32 his3+
	Py 386	h- chp1::chp1-CDΔ-6xmyc-LEU2 ura4D18 ade6-210 leu1-32 arg3D his3D
	Py 3107	h- chp1::V24Rchp1-6xmyc-LEU2 ura4D18 ade6-210 leu1-32 arg3D his3D
	Py 631	h-chp1::N59Achp1-6xmyc-LEU2 ura4D18 ade6-210 leu1-32
	Py 630	h- chp1::V24Mchp1-6xmyc-LEU2 ura4D18 ade6-210 leu1-32
	Py 760	h- chp1::E23Vchp1-6xmyc-LEU2 ura4DS/E ade6-210 leu1-32 arg3D his3D
	Py 1681	h- chp1::E23V,V24Mchp1-6xmyc-LEU2 ura4D18 ade6-210 leu1-32 arg3D his3D
	Py 3086	h- chp1::V21Achp1-6xmyc-LEU2 ura4D18 ade6-210 leu1-32 arg3D his3D
	Py 3141	h- chp1::F61A chp1-6xmyc-LEU2 ura4D18 ade6-210 leu1-32 arg3D his3D
	Py 3091	h- chp1::D48S,D51Schp1-6xmyc-LEU2 ura4D18 ade6-210 leu1-32 arg3D his3D
	Py 3393	h- chp1::chp1$_{aa1-8}$Swi6CD$_{aa68-132}$chp1$_{aa71-960}$-6xmyc-LEU2 ura4D18 ade6-210 leu1-32 arg3D his3D
Fig. 4D	Py 2036	h- otr1R (Sph1)::ura4 ura4-DS/E ade6-210 leu1-32
	Py 1162	h+ otr1R (Sph1)::ura4 ura4-DS/E ago1::F276Aago1-KanR ade6-210 leu1-32
	Py 2940	h- otr1R (Sph1)::ura4 ura4D18 chp1::V24Mchp1 ade6-210 leu1-32
	Py 3917	h- otr1R (Sph1)::ura4 ura4-DS/E or D18 ago1::F276Aago1-KanR chp1::V24Mchp1 ade6-210 leu1-32
	Py 2561	h- otr1R (Sph1)::ura4 ura4-DS/E chp1::E23Vchp1 ade6-210 leu1-32

	Py 3919	h- otr1R (Sph1)::ura4 ura4-DS/E ago1::F276Aago1-KanR chp1::E23Vchp1 ade6-210 leu1-32
	Py 3535	h- otr1R (Sph1)::ura4 ura4DS/E chp1::F61Achp1 ade6-210 leu1-32 arg3D his3D
	Py 3921	h+ otr1R (Sph1)::ura4 ura4DS/E ago1::F276Aago1-KanR chp1::F61Achp1 ade6-210, leu1-32
Fig. 5, 6A, 6B, S9,S10	Py 2036	h- otr1R (Sph1)::ura4 ura4-DS/E ade6-210 leu1-32
	Py 1838	h- otr1R (Sph1)::ura4 ura4DS/E clr4Δ::KanR ade6-210 leu1-32 his3D
	Py 3417	h- otr1R (Sph1)::ura4 ura4-DS/E JP1084 his3+ genomic Clr4 (HpaI)::clr4Δ::KanR ade6-210 leu1-32 his3D
	Py 3413	h- otr1R (Sph1)::ura4 ura4-DS/E chp1::V24Mchp1 JP1084 his3+ genomic Clr4 (HpaI)::clr4Δ::KanR ade6-210 leu1-32 his3D
	Py 3409	h- otr1R (Sph1)::ura4 ura4-DS/E chp1::E23Vchp1 JP1084 his3+ genomic Clr4 (HpaI)::clr4Δ::KanR ade6-210 leu1-32 his3D
	Py 3429	h- otr1R (Sph1)::ura4 ura4-DS/E chp1::N59Achp1 JP1084 his3+ genomic Clr4 (HpaI)::clr4Δ::KanR ade6-210 leu1-32 his3D
	Py 3421	h- otr1R (Sph1)::ura4 ura4-DS/E chp1::F61Achp1 JP1084 his3+ genomic Clr4 (HpaI)::clr4Δ::KanR ade6-210 leu1-32 his3D
	Py 3401	h- otr1R (Sph1)::ura4 ura4-DS/E chp1::D48S,D51Schp1 JP1084 his3+ genomic Clr4 (HpaI)::clr4Δ::KanR ade6-210 leu1-32 his3D
	Py 3425	h- otr1R (Sph1)::ura4 ura4-DS/E chp1::chp1$_{aa1-8}$Swi6CD$_{aa68-132}$chp1$_{aa71-960}$ JP1084 his3+ genomic Clr4 (HpaI)::clr4Δ::KanR ade6-210 leu1-32 his3D
Fig. 6C	Py 3909	h- otr1R Sph1::ura4 ura4-DS/E clr4Δ::KanR ade6-210 leu1-32 his3D + JP1049 (his3+)
	Py 3911	h- otr1R Sph1::ura4 ura4-DS/E clr4Δ::KanR ade6-210 leu1-32 his3D + JP1078 (his3+)
	Py 3912	h- otr1R Sph1::ura4 ura4-DS/E clr4Δ::KanR ade6-210 leu1-32 his3D + JP1078 (his3+)
	Py 3913	h- otr1R Sph1::ura4 ura4-DS/E clr4Δ::KanR chp1::V24Mchp1 ade6-210 leu1-32 his3D + JP1078 (his3+)
	Py 3914	h- otr1R Sph1::ura4 ura4-DS/E clr4Δ::KanR chp1::V24Mchp1 ade6-210 leu1-32 his3D + JP1078 (his3+)
	Py 3915	h- otr1R Sph1::ura4 ura4-DS/E clr4Δ::KanR chp1::E23Vchp1 ade6-210 leu1-32 his3D + JP1078 (his3+)
	Py 3916	h- otr1R Sph1::ura4 ura4-DS/E clr4Δ::KanR chp1::E23Vchp1 ade6-210 leu1-32 his3D + JP1078 (his3+)
Fig. S6C	Py 42	h- ura4-D18 ade6-210 leu1-32 arg3D his3D
	Py 1080	h- tas3::tas3-TAP-KanR chp1::chp1-6xmyc-LEU2+ ade6-210 leu1-32 arg3D? his3D? ura4D18 or DS/E
	Py 3562	h- chp1::F61Achp1 tas3::tas3-TAP-KanR ade6-210 leu1-32 ura4DS/E arg3D? his3D?
	Py 3575	h- chp1::E23Vchp1 tas3::tas3-TAP-KanR ade6-210 leu1-32 ura4DS/E or D18 arg3D?his3D?
Fig. S8	Py 3494	h- otr1R Sph1::ura4 ura4-DS/E tas3::tas3-TAP-KanR ade6-210 leu1-32 arg3D? his3D?
	Py 3497	h- otr1R Sph1::ura4 ura4-DS/E tas3::tas3 W265A,G266A-TAP-KanR ade6-210 leu1-32 arg3D? his3D
	Py 4057	h- otr1R Sph1::ura4 ura4-DS/E chp1::E23Vchp1 tas3::tas3-TAP-KanR ade6-210 leu1-32 his3D?
	Py 4058	h- otr1R Sph1::ura4 ura4-DS/E chp1::N59Achp1 tas3::tas3-TAP-KanR ade6-210 leu1-32 his3D arg3?
	Py 4062	h- otr1R Sph1::ura4 ura4-DS/E chp1::E23Vchp1 tas3::tas3 W265A,G266A-TAP-KanR ade6-210 leu1-32 his3?
	Py 4064	h- otr1R Sph1::ura4 ura4-DS/E chp1::N59Achp1 tas3::tas3 W265A,G266A-TAP-KanR ade6-210 leu1-32 his3D arg3?

	PY1402	h- otr1R Sph1::ura4 ura4-DS/E tas3::KanR ade6-210 leu1-32
methods	Py 282	h- chp1::chp1CDΔ::ura4+-6xmyc-LEU2 ura4D18 ade6-210 leu1-32 arg3D his3D
methods	Py 3054	h- chp1::chp1CDΔ::ura4+ ura4D18 ade6-210 leu1-32 arg3D his3D

Schalch et al., Figure S1

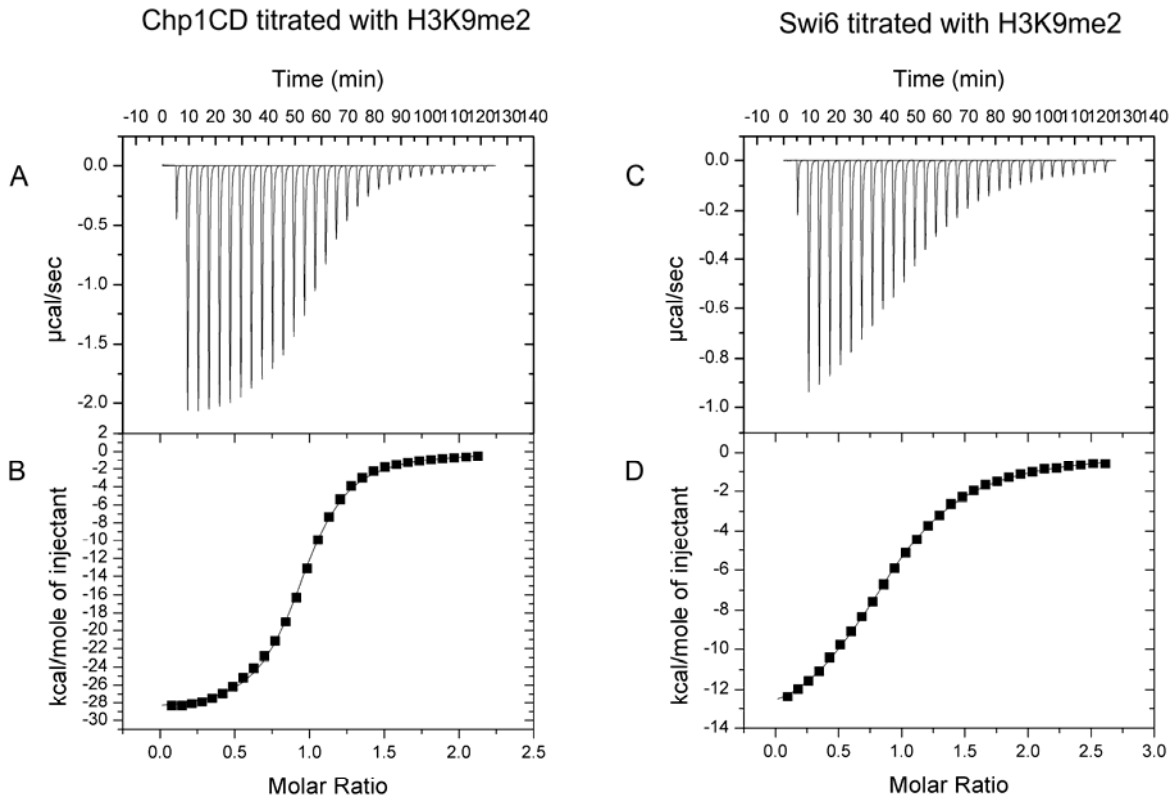

Figure S1. Isothermal titration calorimetry of Chp1 CD and Swi6 binding to H3K9me2 peptides. A. Raw data for heats measured upon injections of H3 peptide (H3K9me2) to Chp1 chromodomain as described in experimental procedures. **B.** Integrated heats of the injections for Chp1 with the best fit for the data corresponding to the solid line. **C.** Raw data for heats measured upon injections of H3 peptide (H3K9me2) to Swi6. **D.** Integrated heats of the injections for Swi6 with the best fit for the data corresponding to the solid line. Binding curves were analyzed by non-linear least squares fitting of the data using the Origin (MicroCal) software package.

Schalch et al., Fig. S2

A.

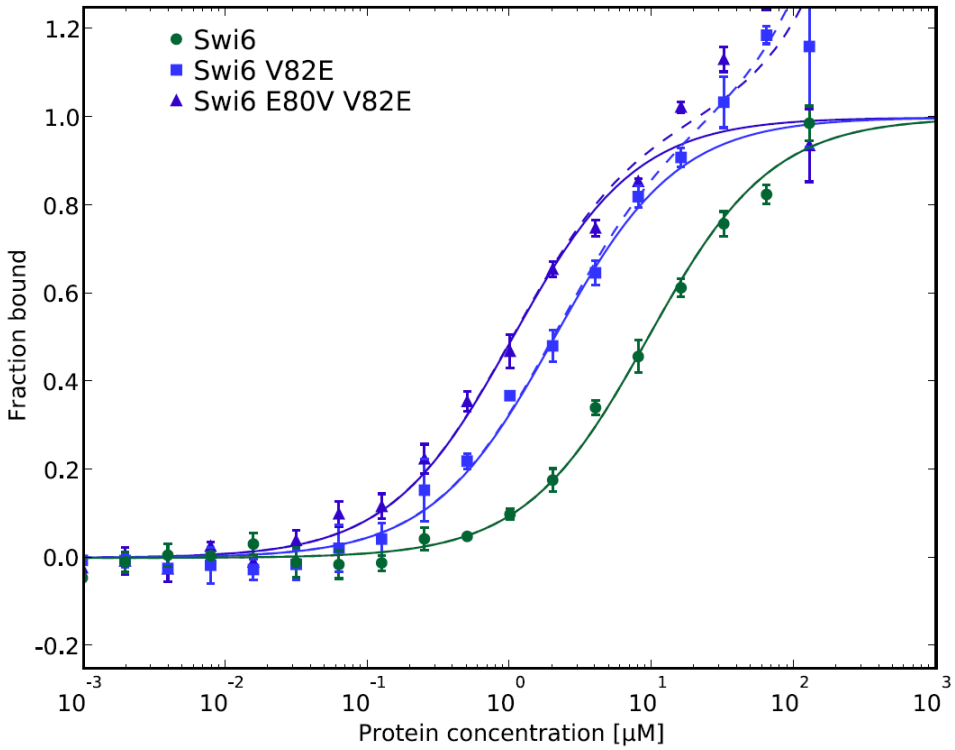

B.

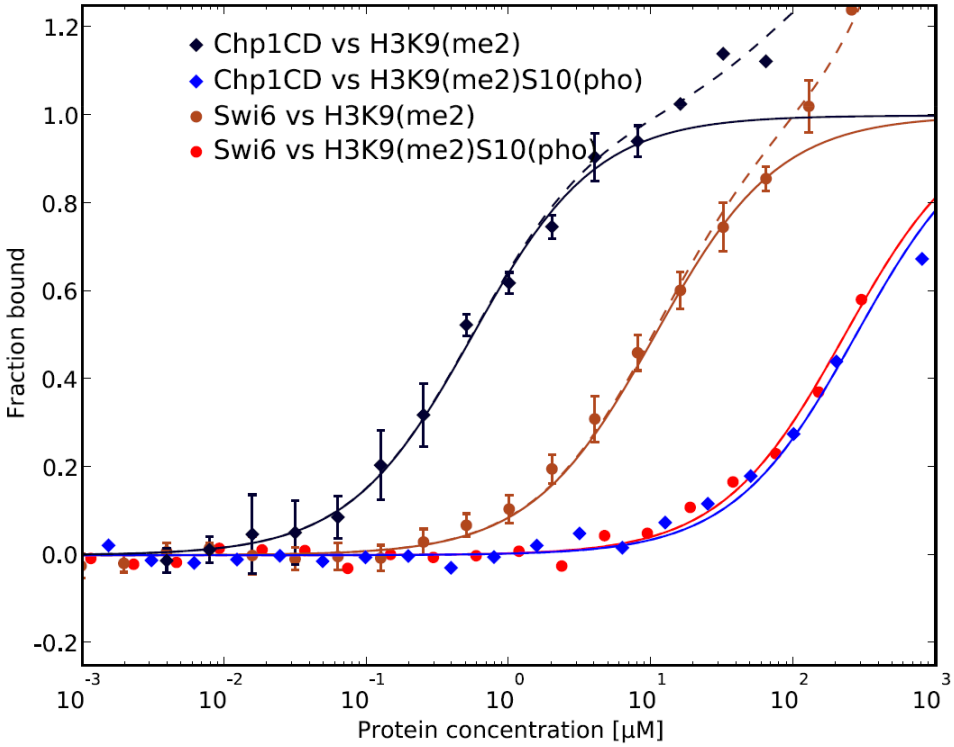

Figure S2. A. Affinity measurements for binding of Swi6 V82E and Swi6 E80V, V82E to fluorescein labeled H3K9me2 peptide by fluorescence polarization. **B.** Affinity measurements for binding of Swi6 and Chp1 CD to fluorescein labeled H3K9me2 and H3K9me2S10P peptides by fluorescence polarization. Data for binding to non phosphorylated peptides in Fig. S2B is taken from Figure 1. For both figures, error bars indicate standard deviation of 3 or more measurements. Solid lines represent fit for specific binding, dashed lines include fit for non-specific binding.

Schalch et al., Fig. S3

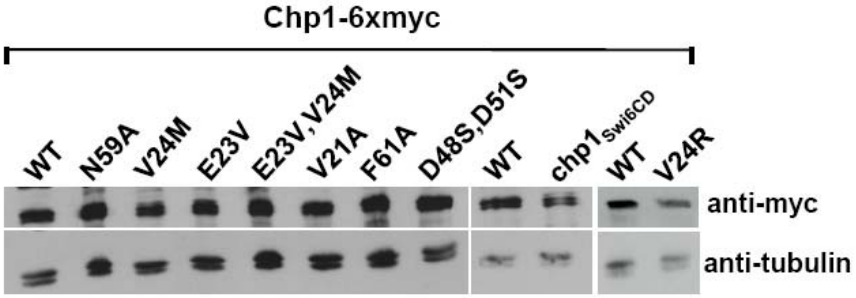

Figure S3. Western analysis of steady state expression levels of mutants engineered into the genomic *chp1-6xmyc* tagged locus detected with anti-myc antibody, and compared with α-tubulin levels (revealed with anti-TAT1 antibody) as loading control. Strains used were PY 189, 631, 630, 760, 1681, 3086, 3141, 3091, 3393, 3107.

Schalch et al., Fig. S4

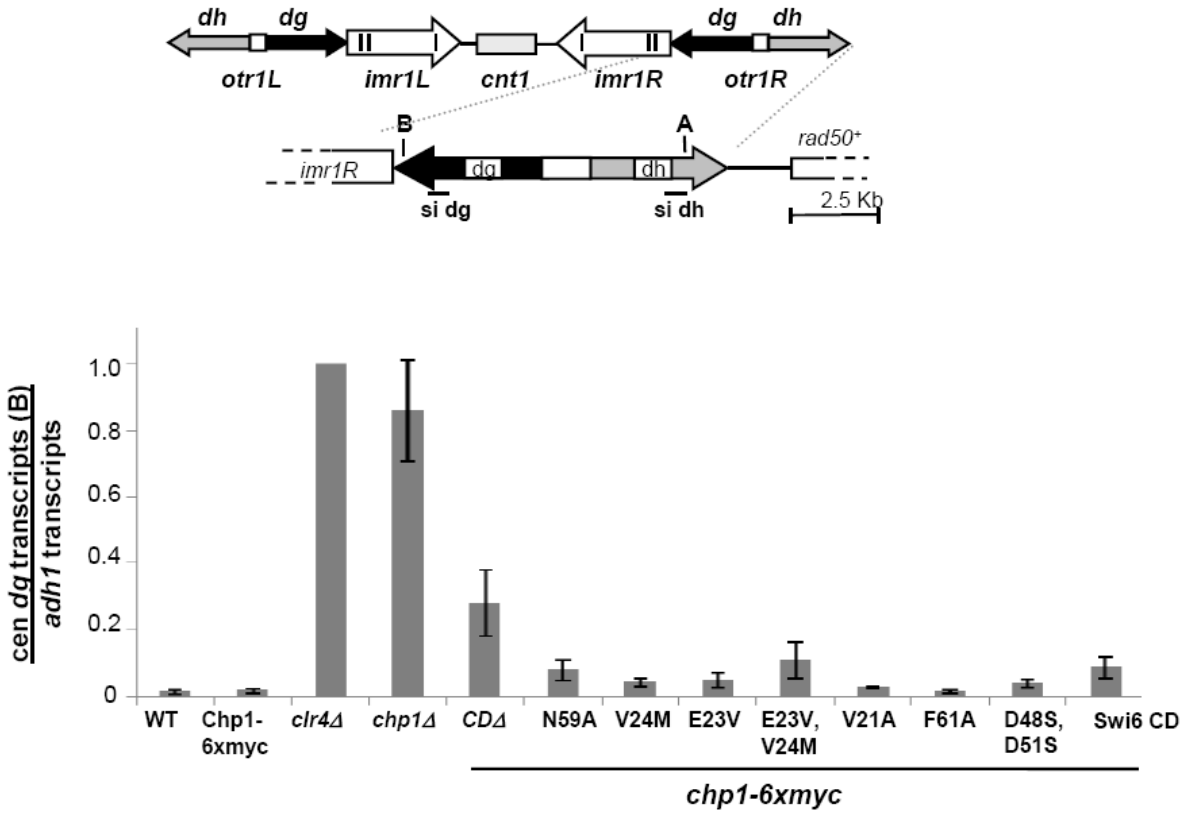

Figure S4. Real time PCR analysis of centromeric sequence representation (sites B in dg) relative to *adh1* in cDNA generated by random priming from RNA derived from *chp1*+, *chp1* null, *clr4* null or *chp1-6xmyc* mutant strains (PY42, 189, 1798, 90, 386, 631, 630, 760, 1681, 3086, 3141, 3091, 3393). Data are represented as mean +/- SEM, after normalization to transcript levels in *clr4* null cells, which was set at 1.

Schalch et al. Fig. S5

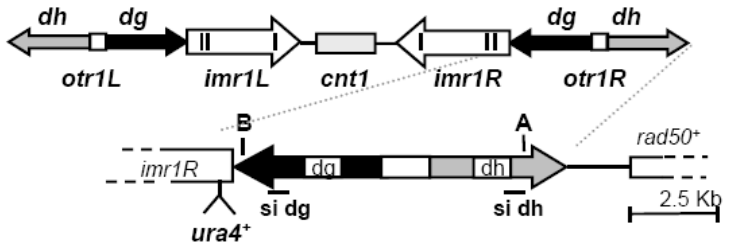

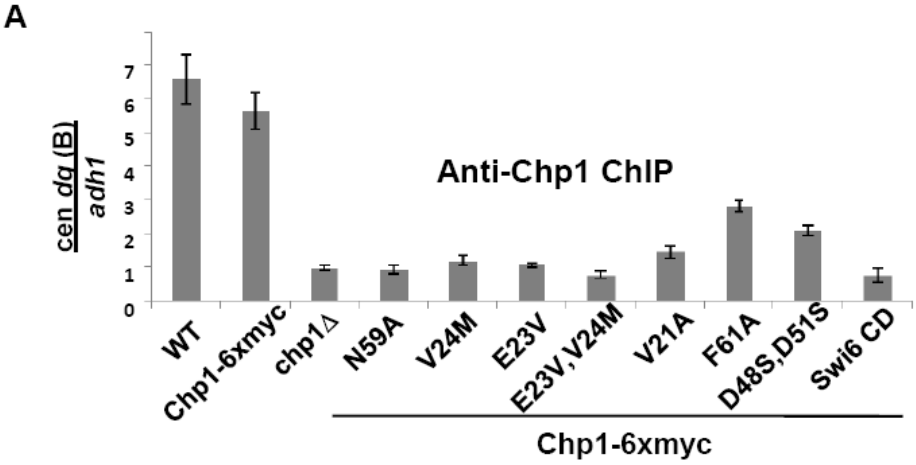

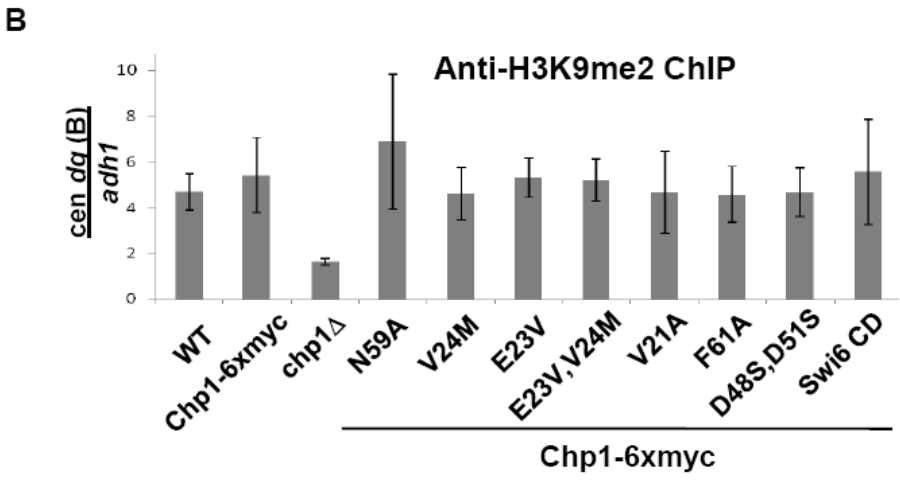

Figure S5A. ChIP analysis of Chp1 association with centromeric repeat dg sequences in strains bearing chromodomain mutations in Chp1, normalized to the euchromatic *adh1* sequence, and to the signal obtained from *chp1* null cells, which was set at 1. Strains used in analysis were PY42, 189, 1798, 90, 631, 630, 760, 1681, 3086, 3141, 3091, 3393. Data were obtained by real-time PCR and are represented as mean +/- SEM.
Figure S5B. ChIP analysis of H3K9me2 association with the dg regions of the centromere, relative to *adh1*, measured by real-time PCR. Values obtained were normalized to the value obtained from a *clr4* null strain which lacks H3K9me2 (set at 1). Data are represented as mean +/- SEM. Strains used were PY42, 189, 1798, 90, 631, 630, 760, 1681, 3086, 3141, 3091, 3393.

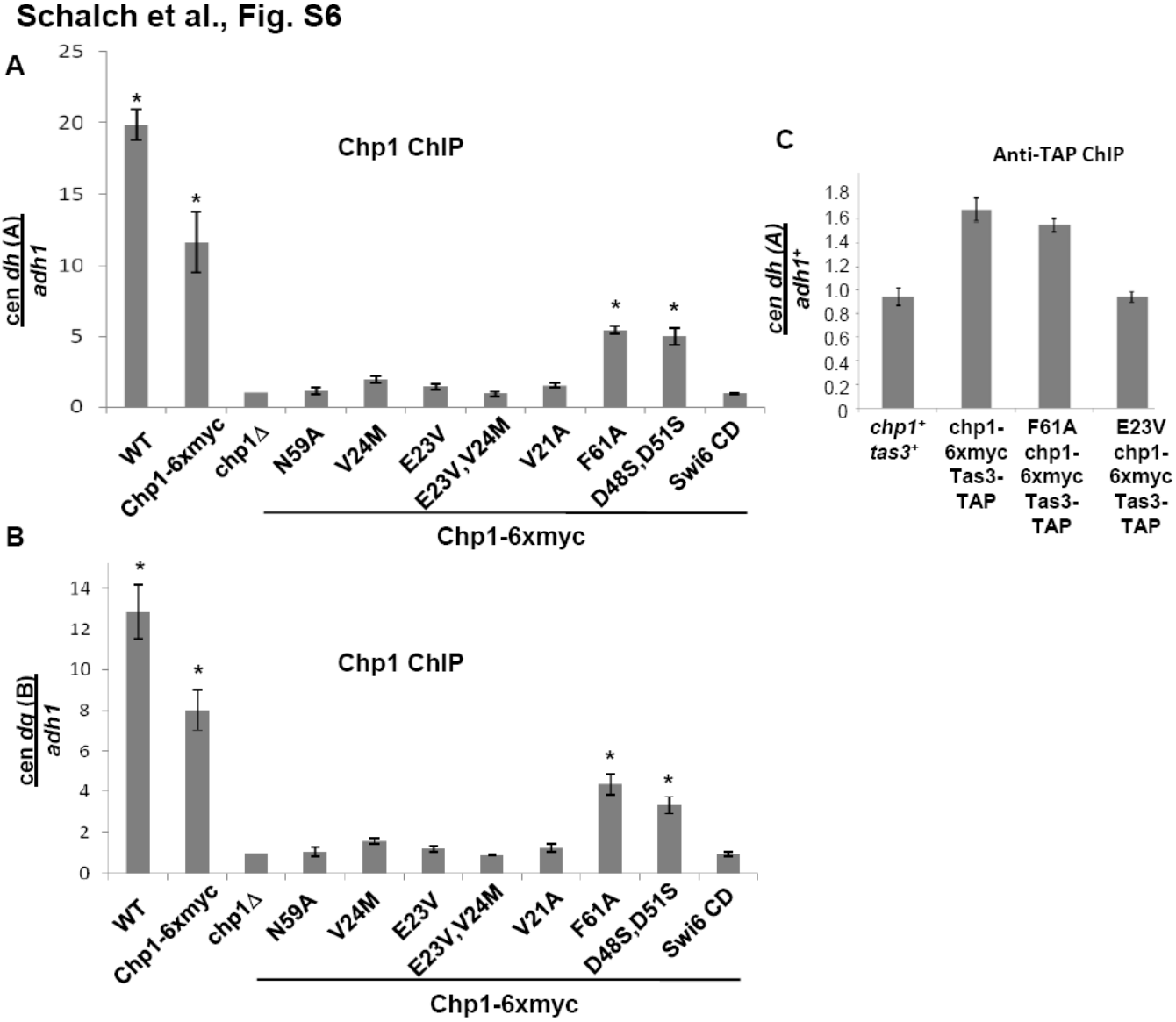

Figure S6A. ChIP analysis of Chp1 association with centromeric repeat sequences (dh site A) relative to *adh1* in cells that have been fixed with both 3% PFA and 5mM DMA. Strains used were PY42, 189, 90, 631, 630, 760, 1681, 3086, 3141, 3091, 3393, and these were also used for Fig. S6B. Data are normalized to the values obtained for the *chp1* null strain, which was set at 1, and represent the mean +/- SEM of 4 experiments. Values that differ significantly from *chp1* null, by Anova test ($p<0.01$), are marked with asterisk.

Figure S6B. ChIP analysis of Chp1 association with centromeric repeat sequences (dg-site B) relative to *adh1* in doubly fixed cells as above. Data are normalized to 1 for the *chp1* null control, and represent mean +/- SEM of real-time PCR analyses. Values that differ significantly from *chp1* null, by Anova test ($p<0.01$), are marked with asterisk.

Figure S6C. ChIP analysis of Tas3-TAP association with centromeres (dh-site A) in strains expressing Chp1 chromodomain mutants. Strains used were Py42, 1080, 3562, 3575.

Schalch et al., Fig. S7

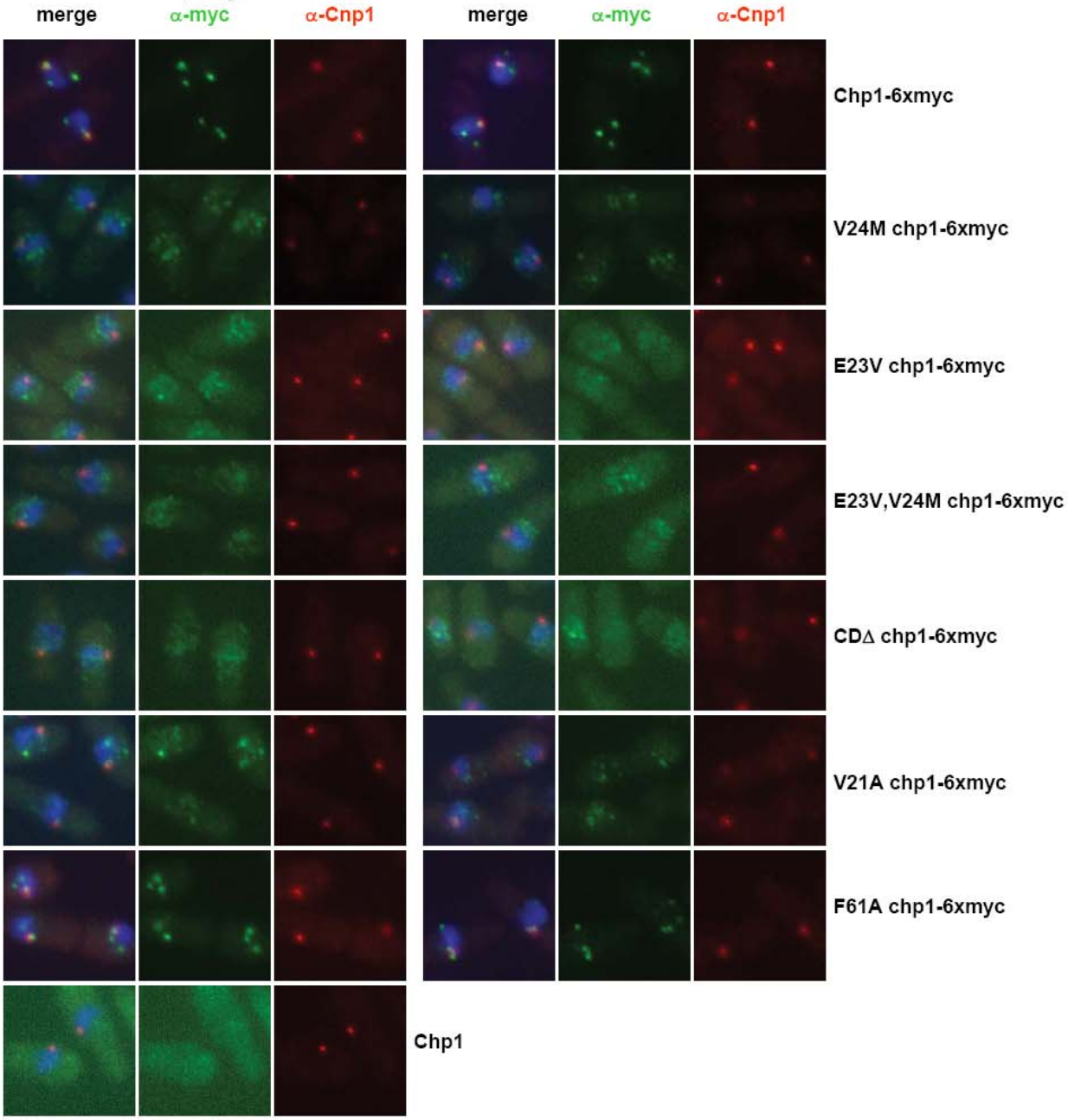

Figure S7. Immunofluorescent localization of Chp1-6xmyc in fixed cells. Antibodies that recognize the myc tagged Chp1 mutants were used in immunofluorescence analyses to monitor protein localization. Chp1 associates with all sites of heterochromatin in wild type cells, and its localization at centromeres can be assessed by co-staining with anti-Cnp1CENP-A antibody that specifically marks kinetochores. In wild type cells, Chp1 stains all three site of heterochromatin including the centromere (Petrie et al 2005, Sadaie et al 2004). F61Achp1 also showed overlap with Cnp1 staining, as did V21Achp1. The other mutants however, that exhibit lower affinity of binding to H3K9me, showed a more delocalized pattern of myc staining, and in these strain backgrounds it was not possible to determine whether the mutant Chp1 was still retained at centromeres. A similar delocalization of staining was seen for ΔCD-chp1-myc, which does not associate with centromeres (Petrie et al 2005). Two fields of cells are shown for each mutant.

Schalch et al. Fig. S8

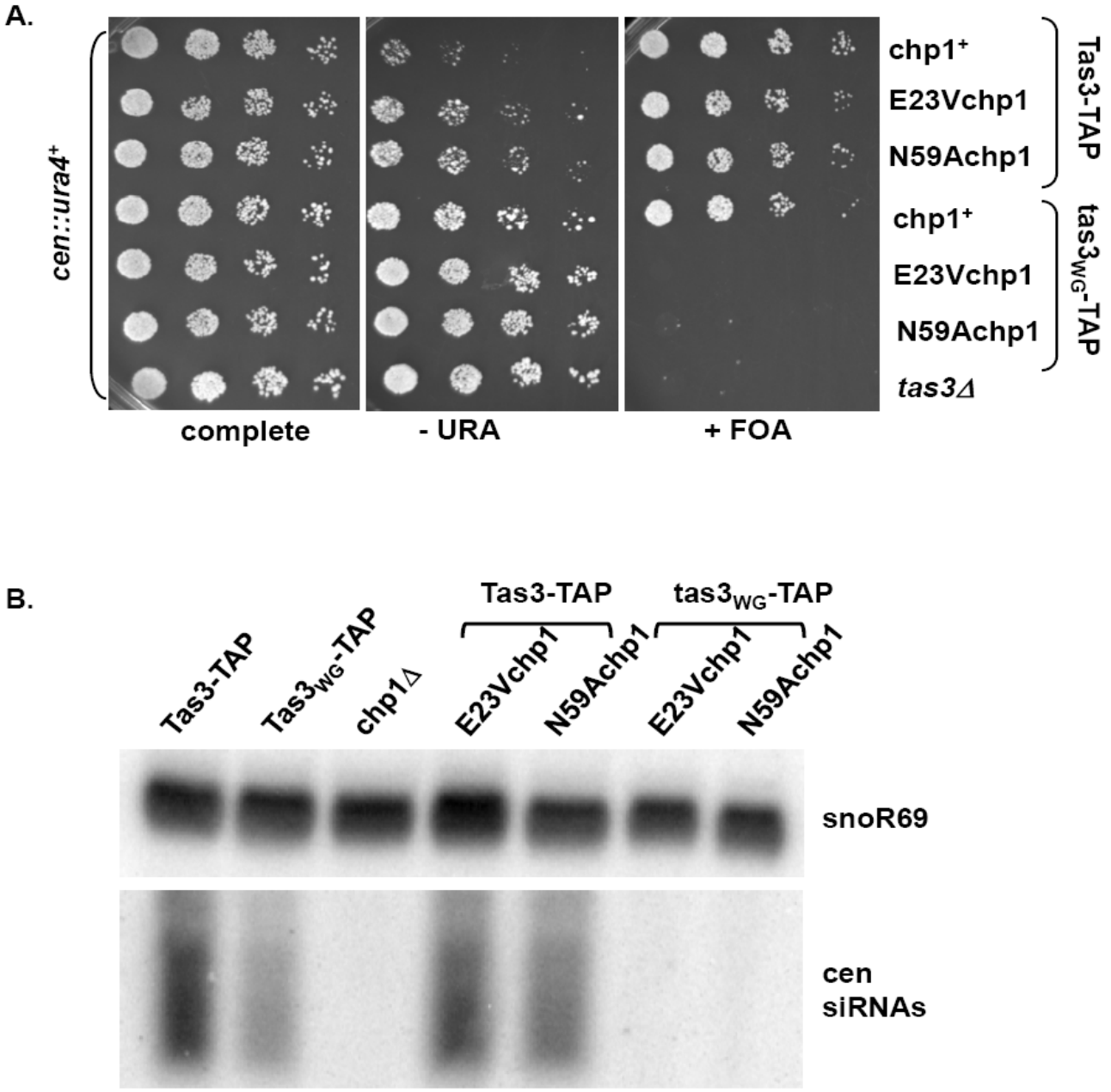

Figure S8. Combination of Chp1 chromodomain mutants with $Tas3_{WG}$ mutant causes loss of maintenance of centromeric heterochromatin. **A.** Serial dilution assay of cells bearing *ura4* transgene inserted within outer repeats of centromere 1 (*cen::ura4*+) plated on complete media, or media lacking uracil or supplemented with FOA. Cells carried *tas3-TAP* or *tas3$_{WG}$-TAP* alleles, and were wild type for *chp1*, or carried point mutated *chp1* chromodomains. *tas3Δ* cells were used as control. **B.** Northern blot analysis of small RNA purified from strains described above, probed for snoR69 as a control, or centromeric siRNAs derived from both dg and dh repeats. Strains used in these analyses : PY3494, PY3497, PY225, PY4057, PY4058, PY4062, PY4064, PY1402.

Schalch et al., Fig. S9

A

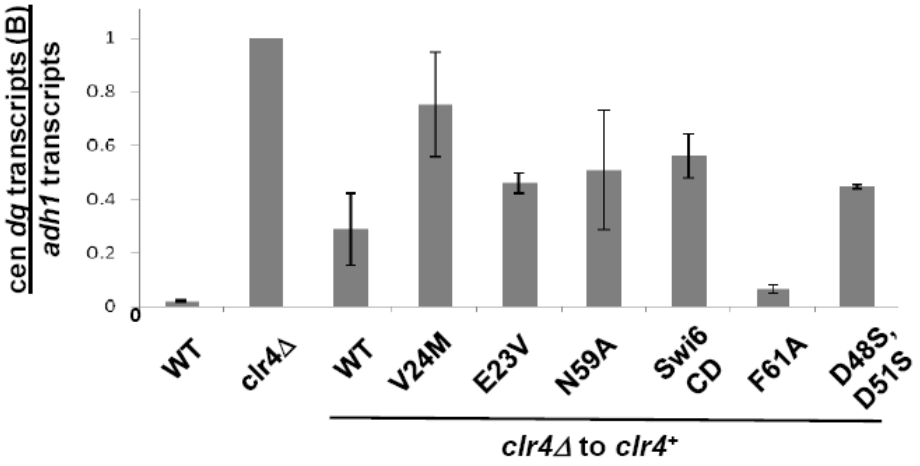

B

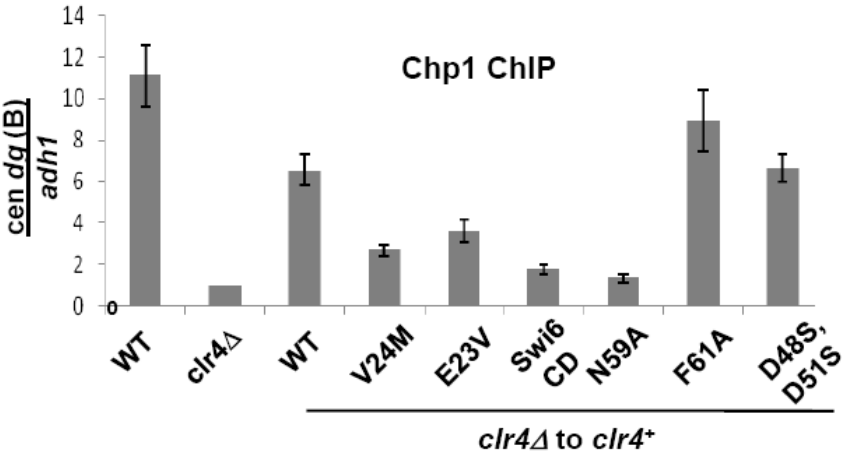

Figure S9A. Real-time PCR analysis of centromeric transcripts from the dg region (B) relative to euchromatic *adh1* transcripts in cDNA prepared by random priming of total RNA. Strains used were PY 2036, 1838, 3417, 3413, 3409, 3429, 3421, 3401, 3425, and these were also used for Fig. S9B. Data are normalized to the values obtained for the *clr4* null strain, which was set at 1, and represent the mean +/- SEM.

Figure S9B. ChIP analysis of Chp1 association with centromeric repeat sequences (dg-site B) relative to *adh1*, in strains in which *clr4* has been reintegrated (*clr4D* to *clr4*+).Data are normalized to 1 for the clr4 null control, and represent mean +/- SEM of real-time PCR analyses.

Schalch et al., Fig. S10

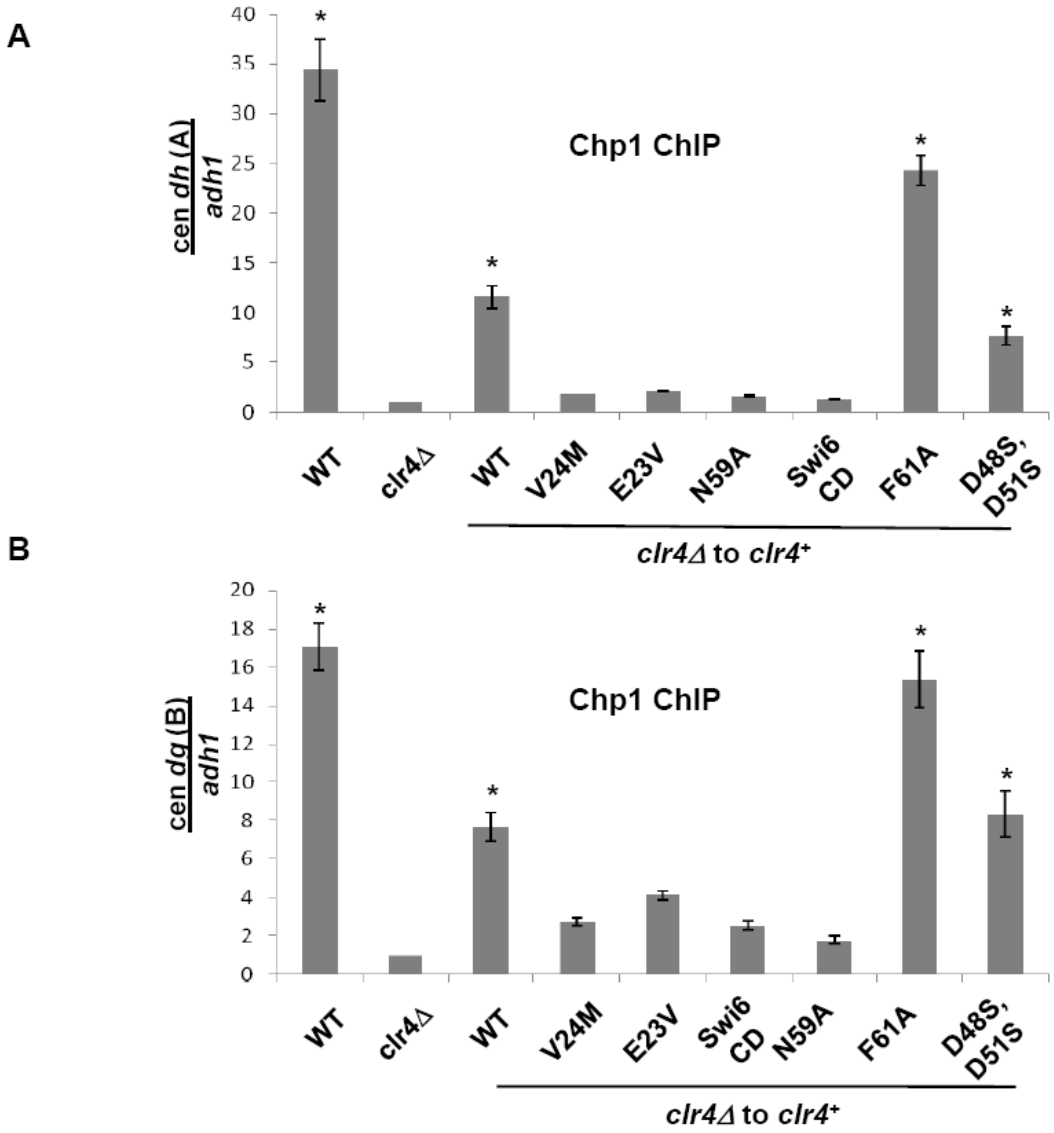

Figure S10A. ChIP analysis of Chp1 association with centromeric repeat sequences (dh site A) relative to *adh1*, in doubly fixed strains in which *clr4* has been reintegrated. Strains used were PY 2036, 1838, 3417, 3413, 3409, 3429, 3421, 3401, 3425, and these were also used for Fig. S10B. Data are normalized to the values obtained for the *clr4* null strain, which was set at 1, and represent the mean +/- SEM of 4 experiments. Asterisks highlight samples giving statistically significant association relative to *clr4* null by Anova test ($p<0.01$).

Figure S10B. ChIP analysis of Chp1 association with centromeric repeat sequences (dg-site B) relative to *adh1*, in doubly fixed strains in which *clr4* has been reintegrated (*clr4Δ* to *clr4*+).Data are normalized to 1 for the *clr4* null control, and represent mean +/- SEM of real-time PCR analyses. Asterisks highlight samples giving statistically significant association relative to *clr4* null by Anova test ($p<0.01$).

Schalch et al., Figure S11

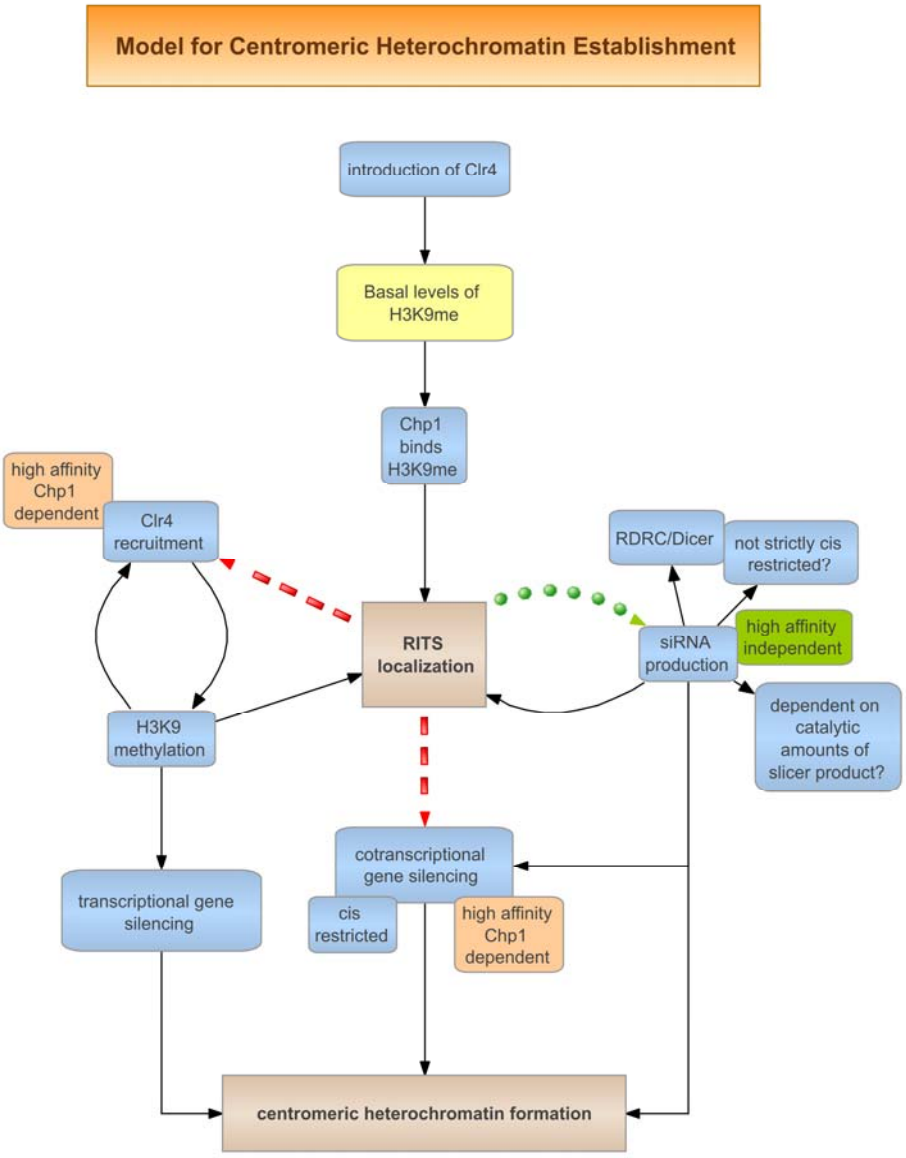

Figure S11. Schematic model of heterochromatin establishment. Red dotted arrows indicate pathways that are blocked in the Chp1 low affinity chromodomain mutants, green dotted arrows indicate pathways that do not depend on high affinity of Chp1.